Utilization Optimization for OVSF Multi-code Assignment in WCDMA Networks[†]

JUI-CHI CHEN[*], HUI-FUANG NG, AND HSIN-LI LIN
Department of Computer Science and Information Engineering, Asia University, Taiwan

ABSTRACT

Radio resources, such as WCDMA OVSF codes, are scarce and valuable in cellular mobile networks, necessitating the need for their efficient use by network operators. Many OVSF code-assignment schemes for WCDMA networks have been widely studied. This paper proposes an evaluation model to accurately predict OVSF multi-code assignment performance in WCDMA networks. Theoretical and simulation results indicate that the proposed analytical model works to evaluate the multi-code assignment performance. Two important performance measures, call blocking probability (CBP) and bandwidth utilization (BU), are then adopted to solve a utilization optimization problem for WCDMA network planning and re-planning. The optimization problem applies a given traffic statistic and a specified maximum CBP constraint to maximize the BU by discovering the optimal number of basic-rate codes in a Node-B. Consequently, the operators will be able to use the results to deploy their codes flexibly, and to improve their profitability.

Key words: mobile networks; WCDMA; OVSF code; multi-code.

1. INTRODUCTION

The third generation (3G) mobile networks are characterized by high throughput, wideband services and flexibility. The Universal Mobile Telecommunication System (UMTS) is one of the major 3G mobile networks being developed within the framework defined by the International Telecommunication Union. In 3G Wideband-CDMA (WCDMA) for UMTS network, orthogonal variable spreading factor (OVSF) code transmission supports various wideband services with low and high data rates (3GPP, 2007; Wan, Shih & Chang, 2003; Adachi, Sawahashi & Suda, 1998). Both the forward and the reverse links in WCDMA can apply only one OVSF code, a single code, or multiple OVSF codes, to match a user-requested data rate (Yen & Tsou, 2004; Chao, Tseng & Wang, 2005; Lee, Lee & Sung, 1999; Karakoc & Kavak, 2007). The OVSF codes in a Node-B (3G base station) are valuable and limited, so 3G operators should utilize them efficiently. A Node-B comprises some cells and an OVSF code-assignment system. Several OVSF code-assignment schemes have been widely studied (Cruz-Perez, Vazquez-Avila, Seguin-Jimenez & Ortigoza-Guerrero, 2006; Chen & Hwang, 2006). However, the OVSF code-assignment system performance has seldom been assessed, especially in terms of the call blocking probability (CBP) and bandwidth utilization (BU). CBP and BU are two significant performance measures for the code-assignment system, which respectively represent the quality

[†] This work was partially supported by the National Science Council under the grants No. NSC 96-2221-E-468-001.
[*] Corresponding author. E-mail: rikki@asia.edu.tw

of service (QoS) for subscribers and the profit of operators. This paper proposes the batch-arrival model $M^{\phi(x)}/M/c/c$ to measure the performance of the OVSF multi-code assignment system, and obtains the expressions of CBP and BU. The OVSF multi-code simulation results agree with the predictions calculated from the proposed model, demonstrating that the model successfully evaluates the system performance. CBP and BU are then adopted to solve a utilization optimization problem for WCDMA network planning and re-planning. The optimization problem applies a given traffic statistic and a specified maximum CBP constraint to maximize the BU by discovering the optimal number of OVSF basic-rate codes in a Node-B. Consequently, operators can use the results to deploy their frequencies or codes flexibly, and to improve their profitability. The proposed model may help to construct the WCDMA networks.

The remainder of this paper is organized as follows. Section 2 describes the OVSF code. Section 3 presents the proposed model, while Section 4 shows the simulation results and verifies the theoretical analysis. Section 5 applies the performance measures to solve the multi-code utilization-optimization problem. A conclusion is provided in Section 6.

2. THE OVSF CODE

2.1 OVSF Code Generation

In WCDMA, two spreading operations are applied to the physical channels. As shown in Figure 1, the first operation is channelization, which transforms every data symbol into a number of chips and supports various wideband services with different data rates. The number of chips per data symbol is called the spreading factor. The channelization codes are OVSF codes that preserve the orthogonality between channels at different rates. As illustrated in Figure 2, a code tree recursively generates the codes based on a modified Walsh-Hadamard transformation (3GPP, 2007). An OVSF code is given by $C_{ch,SF}^{k}$, where SF denotes the spreading factor; k denotes the code number, and $1 \le k \le SF = 2^n$.

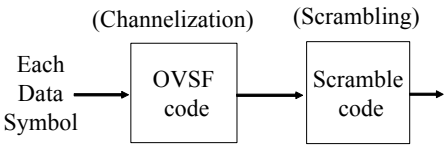

Figure 1. Two spreading operations in WCDMA (3GPP, 2007).

Variable spreading factors are used for the low and medium-high data rates. In the reverse link the spreading factors for data transmission range from 4 to 256, while in the forward link the factors vary from 4 to 512, with restrictions on the use of the factor 512. Upon requiring higher data rates, a user can employ the multicode

transmission and parallel code channels. Up to six parallel codes are used to raise the data rate, which can accommodate 2 Mbps if the coding rate is 1/2. The maximum spreading factor $SF_{\max}$ normally equals the system capacity. Without loss of generality, the data rates described later are normalized by the basic data rate R_b, which denotes an OVSF basic-rate code with $SF_{\max}$. All codes with the same spreading factor SF are located in the same level $log_2(SF)$ in the code tree. Restated, any code in the level $log_2(SF)$ is associated with the data rate $\frac{SF_{\max}}{SF} R_b$.

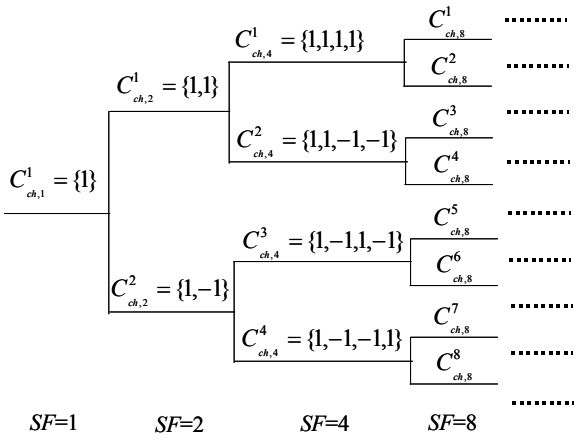

Figure 2. Code tree for generation of the OVSF codes.

2.2 Code-limited Capacity Test

A request rate R_i for call i can generally be expressed as a polynomial, $R_i = \sum_{j=0}^{n} r_j 2^j$, where $r_j \in \{0,1\}$; $n = \log_2(SF_{\max})$; $1 \le R_i \le SF_{\max}$, and R_i is the value of a multiplication of R_b. Before assigning code(s), the Node-B must measure its available system capacity, which can be performed by either of two methods, interference-limited test or code-limited test.

In the code-limited test, the system capacity equals $SF_{\max} \times R_b$ in a single Node-B. The nonblocking condition can then be defined as

$$\sum_{j=1}^{k-1} R_j + R_k \le SF_{\max} \times R_b. \tag{1}$$

The code-limited test is adopted herein. Node-B may run out of codes since the number of OVSF codes is limited. Call i is blocked if the above inequality is not met. CBP denotes the probability of blocking of incoming call requests in a Node-B, denoted as the number of blocked calls divided by the total number of calls during a long period of time. BU represents the utilized rate of total bandwidth in the Node-B, which is defined by

$$\sum_{i=1}^{N} (T_{duration}^{i} \times \frac{SF_{\max}}{SF_i}) \Big/ (T_{total} \times SF_{\max}), \quad (2)$$

where N is the number of successful calls during the total observing time T_{total}, and SF_i is the spreading factor of the successful call i with duration $T_{duration}^{i}$.

2.3 OVSF Single Code and Multi-code

The OVSF code assignment attempts to support as many users as possible. By a single-code assignment scheme, user equipment (UE) transmits its signal on only one channel with a variable data rate, and needs only one RAKE receiver (also called RAKE combiner; briefly called receiver later). A UE equipped with only one receiver can convey only a single-code rate R_i with $\sum_{j=0}^{n} r_j \le 1$. Therefore, the call i with $\sum_{j=0}^{n} r_j > 1$ is assigned with an approximate and slightly higher single-code rate limited in one code, which can be expressed as

$$\xi(R_i) = 2^{\lfloor \log_2(2*R_i - 1) \rfloor}. \quad (3)$$

On the other hand, with a multi-code assignment scheme, each UE uses more than one code to transmit its signal (Yen et al., 2004)(Chao et al., 2005). The multi-code transmission requires multiple receivers in a UE. From some different criteria, one could find that neither the single code assignment nor the multi-code assignment provides obvious superiority (Lee et al., 1999)(Karakoc & Kavak, 2007). A UE equipped with π RAKE receivers can convey a multi-code rate R_i with $\sum_{j=0}^{n} r_j \le \pi$. Thus, the call i with $\sum_{j=0}^{n} r_j > \pi$ is assigned with an approximate and slightly higher multi-code rate limited in π codes, which can be written as

$$\phi(R_i, \pi) = \begin{cases} 0, \text{ if } \pi = 0 \text{ or } R_i = 0 \\ 2^{\lfloor \log_2(2R_i - 1) - 1 \rfloor} + \phi(R_i - 2^{\lfloor \log_2(2R_i - 1) - 1 \rfloor}, \pi - 1), \text{ if } \pi \ge 1, \end{cases} \quad (4)$$

where π equals the number of receivers in a UE. When π = 1, the approximate multi-code rate forms an approximate single-code rate. Restated, $\phi(R_i, 1) = \xi(R_i)$. In summary, call i requesting rate R_i can be assigned with $\phi(R_i, \pi)$ for the multi-code assignment.

3. $M^{\phi(X)}$/M/C/C FOR THE OVSF MULTI-CODE ASSIGNMENT SYSTEM

The number of OVSF codes with the maximum spreading factor $c = SF_{\max}$ generally is the system capacity in a Node-B. That is, a Node-B has in total cR_b rate resources. An OVSF multi-code assignment system in the Node-B can be treated as a multi-channel queue, with c parallel servers. A scenario in which a system customer requests kR_b, who is assigned with an approximate multi-code $\phi(k,\pi)R_b$ denoted by $\phi(k)R_b$, can also be viewed as $\phi(k)$ customers requesting R_b simultaneously; this allows the case to be treated as a batch (group; bulk) arrival. Furthermore, any call served with $\phi(k)R_b$ can be viewed as $\phi(k)$ basic rate calls released simultaneously—all with the same service (call holding) time. In this scenario the case must be treated as a batch service system problem. However, in the interest of taking a long-term average approach and wanting to reduce model complexity, I simulated the $\phi(k)$ basic rate calls as a high rate multicode call, with the added assumption that customers arrive in groups according to a Poisson process with mean group arrival rate λ and probability sequence $\{ x_k \}$ governing group size. Then, $\lambda^k_{\phi(k)}$ represents the batch arrival rate with the group size of Poisson customer stream $\phi(k)$, where $\lambda^k_{\phi(k)} = x_k\lambda$; $\sum_{k=1}^{n} x_k = 1$; $\lambda = \sum_{k=1}^{n} \lambda^k_{\phi(k)}$; $1 \le k \le n \le \phi(n) \le c$, and k, $n \in N$. The average group size is denoted as $\bar{g} = \sum_{k=1}^{n} \phi(k) P(X = k) = \sum_{k=1}^{n} \phi(k) x_k$, where n is the maximum value that a call can request, and $\phi(n)$ denotes the admitted maximum request rate. The service time (call holding time) for all customers is assumed to have independent exponential distribution with parameter $1/\mu$, and the service discipline is first-come-first-serve with respect to the order of arriving groups. Additionally, the system has no buffer (the queue length equals zero), making it a loss system. If a new call finds that the available capacity in the corresponding Node-B cannot satisfy its rate requirement, it is blocked. Hence, the multi-code assignment system can be modeled on the batch-arrival model $M^{\phi(X)}/M/c/c$, whose state-transition diagram is shown in Figure 3. The dotted lines in Figure 3 denote other possible batch arrivals $\lambda^k_{\phi(k)}$.

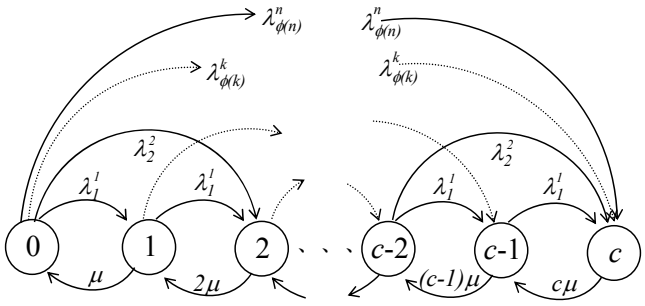

Figure 3. State-transition diagram for the OVSF multi-code assignment system $M^{\phi(X)}/M/c/c$.

First we wish to solve the probability that the number in system $N(t)$ is m at some time t; this we define as

$$P_m(t) = P[N(t) = m], \tag{5}$$

which can be viewed as the transition probability in state m at time t. Each OVSF multi-code call (each group in the proposed model) is independent of others and can request a variable number of basic-rate resources (customers in a group) to meet its data-rate requirement. It is reasonable to assume that the interarrival times between any two continuous calls (groups) have a memoryless negative exponential distribution independent of time t. We also consider the time-independent discrete distribution for the request data rates (group size), such as the geometric distribution. Moreover, the system capacity (number of states) in a Node-B is limited. Thus the proposed model is assumed to be an ergodic continuous time Markov Chain with a finite number of states. Accordingly, we have the resulting differential-difference equations as follows:

$$\frac{dP_o(t)}{dt} = -\lambda P_o(t) + \mu P_1(t), \text{ where } \lambda = \sum_{k=1}^{n} \lambda_{\phi(k)}^{k}, \text{ and } 1 \le n \le \phi(n) \le c; \tag{6}$$

$$\frac{dP_m(t)}{dt} = -\left(m\mu + \sum_{k=1}^{\min[\phi^{-1}(c-m),n]} \lambda_{\phi(k)}^{k} \right) P_m(t) + \sum_{k=1}^{\min[\phi^{-1}(m),n]} \lambda_{\phi(k)}^{k} P_{m-\phi(k)}(t) + (m+1)\mu P_{m+1}(t), \tag{7}$$

where $1 \le m \le c\text{-}1$ and $\phi^{-1}(m) = \phi^{-1}(m, \pi)$ is the maximum h so that $\phi(h, \pi) \le m$.

$$\frac{dP_c(t)}{dt} = -c\mu P_c(t) + \sum_{k=1}^{n} \lambda_{\phi(k)}^{k} P_{c-\phi(k)}(t). \tag{8}$$

Let us define that

$$p_m = \lim_{t \to \infty} P_m(t). \tag{9}$$

Accepting the existence of the limit in (9), we may then set $\lim dP_m(t)/dt$ as $t \to \infty$ equal to zero and immediately derive the result

$$0 = -\lambda p_o + \mu p_1, \quad \lambda = \sum_{k=1}^{n} \lambda_{\phi(k)}^{k}; \tag{10}$$

$$0 = -\left(m\mu + \sum_{k=1}^{\min[\phi^{-1}(c-m),n]} \lambda_{\phi(k)}^{k} \right) p_m + \sum_{k=1}^{\min[\phi^{-1}(m),n]} \lambda_{\phi(k)}^{k} p_{m-\phi(k)} + (m+1)\mu p_{m+1}, \quad 1 \le m \le c-1; \tag{11}$$

$$0 = -c\mu p_c + \sum_{k=1}^{n} \lambda_{\phi(k)}^{k} p_{c-\phi(k)}. \tag{12}$$

Then the equilibrium (steady-state) equations written below are used to obtain the equilibrium probabilities p_m for state m of the model:

$$\lambda p_0 = \mu p_1, \tag{13}$$

where $\lambda = \sum_{k=1}^{n} \lambda_{\phi(k)}^{k}$, and $1 \le n \le \phi(n) \le c$;

$$\left(m\mu + \sum_{k=1}^{\min[\phi^{-1}(c-m),n]} \lambda_{\phi(k)}^{k} \right) p_m = \sum_{k=1}^{\min[\phi^{-1}(m),n]} \lambda_{\phi(k)}^{k} p_{m-\phi(k)} + (m+1)\mu p_{m+1}, \tag{14}$$

where $1 \le m \le c-1$ and $\phi^{-1}(m)=\phi^{-1}(m, \pi)$ is the maximum h so that $\phi(h, \pi) \le m$; and

$$c\mu p_c = \sum_{k=1}^{n} \lambda_{\phi(k)}^{k} p_{c-\phi(k)}. \tag{15}$$

Reforming (13), (14), and (15) yields

$$p_1 = p_0 \lambda / \mu, \tag{16}$$

$$p_{m+1} = \left\{ \left(m\mu + \sum_{k=1}^{\min[\phi^{-1}(c-m),n]} \lambda_{\phi(k)}^{k} \right) p_m - \sum_{k=1}^{\min[\phi^{-1}(m),n]} \lambda_{\phi(k)}^{k} p_{m-\phi(k)} \right\} \Big/ (m+1)\mu, \quad 1 \le m \le c-1, \tag{17}$$

$$p_c = \left[\sum_{k=1}^{n} \lambda_{\phi(k)}^{k} p_{c-\phi(k)} \right] \Big/ c\mu, \tag{18}$$

which can be used for verification.

However, the formal closed-form solution for p_m is complicated to express. Moreover, recursive programs cannot always solve the equations because of overabundant recursive levels for large c. Therefore, an iterative computer procedure can be used to derive the solution. Let $p_0^* = 1$; then

$$p_1^* = p_0^*(\lambda/\mu) = \lambda/\mu . \tag{19}$$

$$p_{m+1}^* = \left\{ \left(m\mu + \sum_{k=1}^{\min[\phi^{-1}(c-m),n]} \lambda_{\phi(k)}^k \right) p_m^* - \sum_{k=1}^{\min[\phi^{-1}(m),n]} \lambda_{\phi(k)}^k p_{m-\phi(k)}^* \right\} \Big/ (m+1)\mu, \quad 1 \le m \le c-1 . \tag{20}$$

According to the conservation relation $\sum_{i=0}^{c} p_i = 1$, the equilibrium probabilities of all states can be written as follows:

$$p_m = p_m^* \Big/ \sum_{i=0}^{c} p_i^* , \quad 0 \le m \le c . \tag{21}$$

Once the equilibrium state probabilities are known, the CBP and BU can be derived. Now if a new multi-code call with data rate $\phi(k)$ finds that the available capacity in the corresponding Node-B cannot satisfy its rate requirement, then it is blocked. Hence the CBP of the proposed model can be expressed as

$$\Omega^{MC} = \sum_{i=0}^{\phi(n)-1} \left(P_{c-i} \sum_{k=\phi^{-1}(i)+1}^{n} \lambda_{\phi(k)}^k \Big/ \lambda \right) , \tag{22}$$

where $1 \le k \le n \le \phi(n) \le c$, $c = SF_{\max}$, $\pi \ge 1$, and $\lambda = \sum_{k=1}^{n} \lambda_{\phi(k)}^k$.

The average number of customers (average system length; ASL) in the proposed model is

$$L_s^{MC} = \lim_{t\to\infty} N(t) = \sum_{i=0}^{c} i p_i . \tag{23}$$

This equals the mean number of busy servers in the model, because the queue size equals zero.

When the system is observed for a long period of time, the average BU can be written as follows:

$$\Psi_1^{MC} = \lim_{T\to\infty} \frac{\sum_{k=1}^{n} \left[\lambda_{\phi(k)}^k T(1 - \sum_{i=c-\phi(k)+1}^{c} p_i) \cdot \phi(k) \cdot \frac{1}{\mu} \right]}{T \cdot c} \overset{\text{L'Hospital's rule}}{=} \frac{\sum_{k=1}^{n} \left[\phi(k) \lambda_{\phi(k)}^k (1 - \sum_{i=c-\phi(k)+1}^{c} p_i) \right]}{c\mu} , \tag{24}$$

where $\sum_{k=1}^{n}\left[\phi(k)\lambda_{\phi(k)}^{k}(1-\sum_{i=c-\phi(k)+1}^{c}p_i)\right]=\bar{g}\lambda_{eff}$, and $1 \le n \le \phi(n) \le c$. Period T has $\lambda_{\phi(k)}^{k}T$ calls with $\phi(k)R_b$ incoming, and thus a total of $\lambda_{\phi(k)}^{k}T(1-\sum_{i=c-\phi(k)+1}^{c}p_i)$ rate-$\phi(k)$ calls are served. The rate-$\phi(k)$ bandwidth usage is given by $\lambda_{\phi(k)}^{k}T(1-\sum_{i=c-\phi(k)+1}^{c}p_i)\phi(k)\frac{1}{\mu}$. Therefore, $\sum_{k=1}^{n}\left[\lambda_{\phi(k)}^{k}T(1-\sum_{i=c-\phi(k)+1}^{c}p_i)\phi(k)\frac{1}{\mu}\right]$ is the total usage of all possible successful multi-code users in the period T, where $1/\mu$ is the mean call holding time. The numerical analysis demonstrates that

$$\Psi_2^{MC}=L_s^{MC}/c=\Psi_1^{MC}. \tag{25}$$

Moreover, the average waiting time in system (system delay) is shown as

$$W_s^{MC}=\frac{L_s^{MC}}{\bar{g}\lambda_{eff}}=L_s^{MC}\Big/\sum_{k=1}^{n}\left[\phi(k)\lambda_{\phi(k)}^{k}(1-\sum_{i=c-\phi(k)+1}^{c}p_i)\right]=1/\mu, \tag{26}$$

which follows Little's rule.

4. THEORETICAL AND SIMULATION RESULTS

To realize the practicability of the proposed model, we simulated the 3G WCDMA channelization environment. The simulated environment consists of a Node-B with an OVSF code table and an OVSF multi-code assignment system, several UEs with various multimedia transmission requirements, a traffic generator, and a statistic recorder. Assume that a π RAKE receiver is embedded in each UE. The Node-B has a limited capacity cR_b bps and code table size c (maximum spreading factor). The system capacity test is code-limited. The traffic generator generates call requests with various data rates and call durations according to the following parameters. Call arrival process is Poisson with mean arrival rate λ calls per unit time, that is, the interarrival time follows a negative exponential distribution with mean $1/\lambda$ units of time. Call duration (call holding time) has a negative exponential distribution with mean $1/\mu$ units of time. The transmission rate (group size) for each call request follows some discrete distribution with mean $\bar{g}R_b$ bps and varies between $1R_b$ and $\phi(n)R_b$ bps. Each simulation ran with over 1,000,000 calls to collect and average the long-term CBP, BU, and other metric values.

The theoretical analysis of the proposed model and the simulation result of the OVSF multi-code assignment system were compared for two cases in which the arriving group size has a discrete uniform distribution (DUNI) and a geometric distribution (GEOM). Any countable distributions, e.g., constant, discrete uniform,

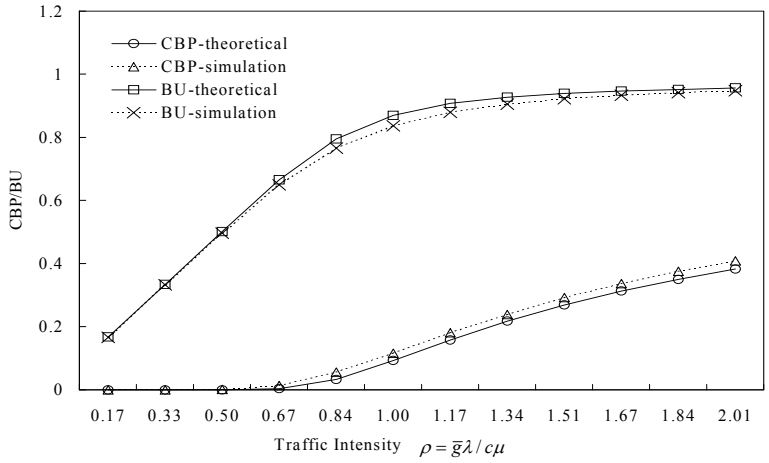

Figure 4. Performance comparison between theoretical and simulation CBP and BU results for the multi-code assignment model, where c = 256; n = 16; μ = 0.00125, and $\bar{g}$ =8.5625.

and geometric distributions, can be applied to map the behavior of the arriving group size. Additionally, call *i* requesting rate R_i is assigned the OVSF multi-code rate $\phi(R_i, \pi)$. That is, the behavior of R_i corresponds to the arriving (requested) group-size distribution, while the behavior of $\phi(R_i, \pi)$ corresponds to the served (assigned) group-size distribution. Of course, the system has offered load $\bar{g}\lambda / \mu$ and traffic intensity $\rho = \bar{g}\lambda / c\mu$.

4.1 Batch-Arrival Size in Discrete Uniform Distribution (DUNI)

The CBP and BU were simulated and calculated by various values of ρ ranging from 0.17 to 2.01, where $\pi = 3$; $c = 256$; $\mu = 0.00125$, and $0.00625 \leq \lambda \leq 0.075$. Such small λ and μ values were adopted to obtain accurate simulation results. High values of λ and μ with the same ratio still result in the same outcome for theoretical analysis. Here the arriving group size was distributed with DUNI, where the maximum arriving group size was $n = 16$; the maximum served group size was $\phi(n, \pi) = \phi(n, 3) = 16$, and the average served group size was $\bar{g} = 8.5625$ (the normalized mean). Figure 4 compares the theoretical and simulated CBP and BU results, where the horizontal axis denotes the traffic intensity given by $\rho = \bar{g}\lambda / c\mu$; the vertical axis shows the CBP and BU. The theoretical CBP and BU values are presented as solid lines with squares and circles, while the simulation CBP and BU are shown as dotted lines with cross signs and plus signs. As shown in Figure 4, both the CBP and the BU increase with rising ρ. Figure 4 also indicates that the theoretical results are close to the simulation results. The analytical results demonstrate that the proposed model works to evaluate the multi-code assignment

Table 1. *Comparison for CBP and BU between theoretical (theo.) and simulation (simu.) results by DUNI group-size distribution, where n = 16; c = 32; π = 1, and $\bar{g}$ = 10.6875*

	CBP		BU		
ρ	theo. Ω^{MC}	simu.	theo. Ψ_1^{MC}	theo. Ψ_2^{MC}	simu.
1.67	0.4533706	0.4929582	0.6386100	0.6386100	0.6557618
3.34	0.5921804	0.6383499	0.7297152	0.7297152	0.7634075
5.01	0.6581966	0.7045222	0.7754196	0.7754196	0.8096241
6.68	0.7006327	0.7428807	0.8057806	0.8057806	0.8359422
8.35	0.7310879	0.7702205	0.8274466	0.8274466	0.8541941
10.02	0.7541610	0.7907782	0.8435782	0.8435782	0.8682929
11.69	0.7723107	0.8054424	0.8560649	0.8560649	0.8789785
13.36	0.7870298	0.8186874	0.8660813	0.8660813	0.8872933
15.03	0.7992773	0.8299386	0.8743674	0.8743674	0.8947071
16.70	0.8096903	0.8370660	0.8813983	0.8813983	0.9002984
18.37	0.8187039	0.8449623	0.8874866	0.8874866	0.9047978
20.04	0.8266231	0.8514409	0.8928437	0.8928437	0.9092839

system. Table 1 presents another numerical comparison data between the theoretical analysis and the simulation, where n = 16; c = 32; π = 1, and $\bar{g}$ = 10.6875.

4.2 Batch-arrival Size in Geometric Distribution (GEOM)

The arriving group size was assumed herein to have a GEOM distribution, where n = 16; c = 64; $\bar{g}$ = 5.01034; π = 2; μ = 0.00125, and λ varies from 0.00625 to 0.075. Table 2 lists the normalized probability of GEOM P_k (from P_1 to P_{16}), because n = 16; the multi-code mapping from the arriving group size k to the served group size $\phi(k)$, and the different values of $\bar{g}$ with various values of π. Table 3 compares the CBP and BU values of the theoretical analysis and simulation. The results demonstrate that the theoretical analysis has approximate values as good as those of the simulation. Thus, the proposed model can be applied to the OVSF multi-code system to analyze its performance accurately. Correspondingly, given c = 128, π = 3, and $\bar{g}$ = 4.84831, Table 4 compares the other theoretical measures with the simulation, including the theoretical BU Ψ_1^{MC}, the theoretical BU L_s^{MC}/c, the average number of busy servers L_s^{MC} and the average system delay W_s^{MC}.

However, results from a comparison of theoretical and simulated CBP and BU are shown in Tables 1 and 3 and Figure 4; the data indicate a strong similarity between the simulation and theoretical results. According to the Poisson Arrival See Time Average property, $\phi(k)$ basic rate calls with identical exponential service times can also be viewed as a single call with a $\phi(k)$ basic rate. The results indicate that both the theoretical analysis and simulation had good approximate values,

suggesting that the proposed model can be applied to an OVSF multicode assignment system for purposes of performance analysis.

Table 2. *The normalized probability of GEOM P_k and the multi-code mapping from k to $\phi(k)$*

	GEOM	π=1		π=2		π=3	
k	P_k	$\phi(k)$	$\phi(k)\times P_k$	$\phi(k)$	$\phi(k)\times P_k$	$\phi(k)$	$\phi(k)\times P_k$
1	0.18899	1	0.18899	1	0.18899	1	0.18899
2	0.15475	2	0.30949	2	0.30949	2	0.30949
3	0.12663	4	0.50652	3	0.37989	3	0.37989
4	0.10372	4	0.41488	4	0.41488	4	0.41488
5	0.08486	8	0.67892	5	0.42432	5	0.42432
6	0.06949	8	0.55592	6	0.41694	6	0.41694
7	0.05698	8	0.45581	8	0.45581	7	0.39883
8	0.04659	8	0.37271	8	0.37271	8	0.37271
9	0.03812	16	0.61000	9	0.34312	9	0.34312
10	0.03127	16	0.50039	10	0.31274	10	0.31274
11	0.02558	16	0.40935	12	0.30702	11	0.28143
12	0.02094	16	0.33506	12	0.25129	12	0.25129
13	0.01713	16	0.27407	16	0.27407	13	0.22268
14	0.01404	16	0.22464	16	0.22464	14	0.19656
15	0.01149	16	0.18384	16	0.18384	16	0.18384
16	0.00941	16	0.15058	16	0.15058	16	0.15058
Σ	4.83682	$\bar{g}$	6.17116	$\bar{g}$	5.01034	$\bar{g}$	4.84831

Table 3. *Comparison for CBP and BU between theoretical (theo.) and simulation (simu.) results by GEOM group-size distribution, where n = 16; c = 64; π = 2, and $\bar{g}$ = 5.01034*

	CBP		BU		
ρ	theo. Ω^{MC}	simu.	theo. Ψ_1^{MC}	theo. Ψ_2^{MC}	simu.
0.39	0.0030420	0.0101700	0.3886715	0.3886715	0.3760023
0.78	0.0627257	0.0899449	0.6812323	0.6812323	0.6448877
1.17	0.1640328	0.1978408	0.8071766	0.8071766	0.7757729
1.57	0.2516573	0.2890984	0.8612162	0.8612162	0.8417250
1.96	0.3208896	0.3618775	0.8898766	0.8898766	0.8774254
2.35	0.3762396	0.4166558	0.9076730	0.9076730	0.8996837
2.74	0.4215485	0.4614316	0.9199007	0.9199007	0.9141850
3.13	0.4594545	0.4977410	0.9288879	0.9288879	0.9250525
3.52	0.4917529	0.5284554	0.9358142	0.9358142	0.9329997
3.91	0.5196927	0.5554247	0.9413419	0.9413419	0.9395927
4.31	0.5441673	0.5782186	0.9458728	0.9458728	0.9446913
4.70	0.5658330	0.5989240	0.9496653	0.9496653	0.9489072

Table 4. *Comparison for some measures between theoretical and simulation results by GEOM group-size distribution, where c = 128; π = 3, and $\bar{g}$ = 4.84831*

ρ	Ψ_1^{MC}	Ψ_2^{MC}	simu. BU	L_s^{MC}	simu. L_s^{MC}	$1/\mu$ W_s^{MC}	simu. W_s^{MC}
0.1894	0.1894	0.1894	0.1859	24.2	23.8	800	799.1
0.3788	0.3788	0.3788	0.3702	48.5	47.4	800	799.1
0.5682	0.5657	0.5657	0.5455	72.4	69.8	800	798.4
0.7575	0.7252	0.7252	0.6894	92.8	88.2	800	797.2
0.9469	0.8244	0.8244	0.7880	105.5	100.8	800	798.9
1.1363	0.8766	0.8766	0.8445	112.2	108.0	800	799.9
1.3257	0.9050	0.9050	0.8801	115.8	112.6	800	799.5
1.5151	0.9221	0.9221	0.9032	118.0	115.5	800	797.6
1.7045	0.9333	0.9333	0.9182	119.5	117.4	800	797.2
1.8939	0.9413	0.9413	0.9303	120.5	119.0	800	799.7
2.0833	0.9473	0.9473	0.9380	121.3	120.0	800	799.1
2.2726	0.9519	0.9519	0.9448	121.8	120.8	800	800.7

5. OVSF MULTI-CODE UTILIZATION OPTIMIZATION

This section examines an optimization problem that finds the optimal number of basic-rate codes c for the OVSF multi-code assignment system in a Node-B to maximize the BU, with a given traffic intensity and a specified maximum CBP constraint. The optimization problem can be described as follows.

Given λ, μ and a CBP constraint C_{Pc}, determine the optimal value of c so as to

$$\text{maximize} \quad \Psi_1^{MC} = \frac{\sum_{k=1}^{n}\left[\phi(k)\lambda_{\phi(k)}^{k}\left(1-\sum_{i=c-\phi(k)+1}^{c} p_i\right)\right]}{c\mu}$$

$$\text{subject to} \quad \lambda > 0, \mu > 0, 1 > C_{Pc} > 0;$$

$$\Omega^{MC} = \sum_{i=0}^{\phi(n)-1}\left(p_{c-i}\sum_{k=\phi^{-1}(i)+1}^{n}\lambda_{\phi(k)}^{k}\Big/\lambda\right) \le C_{Pc},\ c \in N. \tag{27}$$

The monotonicity of CBP and BU in the multi-code assignment system was verified by tracing them using numerical analysis, as depicted in Figure 5, where n = 16; π = 2; λ = 0.00625; μ = 0.00125; the arriving group size was distributed with DUNI; $\bar{g}$ = 9.0, and the offered load was $\bar{g}\lambda/\mu$ = 45. Under the constant offered load, a higher c implies a lower CBP. Nevertheless, the BU may not have the monotonicity under certain offered load, such as 45, as shown in Figure 5. Consequently, the optimization problem is solved by first determining c to maximize the CBP restricted by C_{Pc}, then searching for c increasingly to maximize BU.

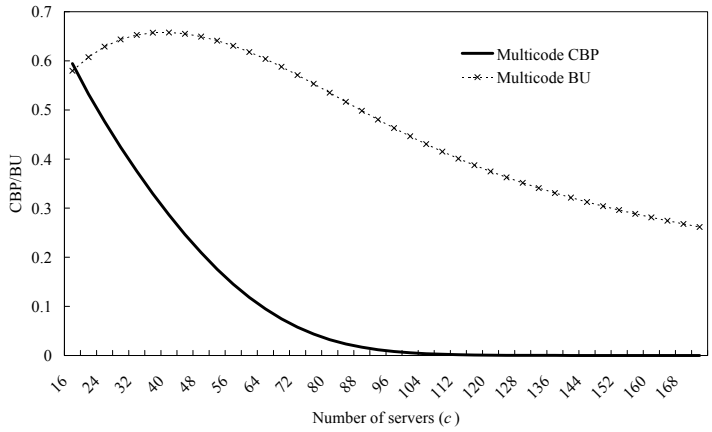

Figure 5. CBP and BU in the OVSF multi-code assignment system when the number of servers c increases.

Table 5. *Optimal values of c for maximizing BU with CBP ≤ 5% (Cp_c = 5%) in various values of the offered load*

Offered load	π	Opt. c	CBP [c-1]	CBP [c]	CBP [c+1]	BU [c-1]	BU [c]	BU [c+1]
30.9	1	53	0.0501	0.0462	0.0425	0.5297	0.5245	0.5192
61.7	1	84	0.0509	0.0481	0.0455	0.6644	0.6606	0.6567
123.4	1	143	0.0518	0.0500	0.0482	0.7767	0.7744	0.7721
185.1	1	202	0.0502	0.0488	0.0475	0.8267	0.8251	0.8235
246.8	1	259	0.0507	0.0496	0.0484	0.8583	0.8571	0.8559
25.1	2	42	0.0549	0.0497	0.0449	0.5387	0.5322	0.5256
50.1	2	68	0.0514	0.0480	0.0447	0.6675	0.6627	0.6579
100.2	2	116	0.0523	0.0500	0.0478	0.7787	0.7758	0.7730
150.3	2	164	0.0506	0.0489	0.0472	0.8281	0.8261	0.8241
200.4	2	211	0.0502	0.0488	0.0474	0.8584	0.8569	0.8554
24.2	3	41	0.0528	0.0475	0.0426	0.5402	0.5332	0.5261
48.5	3	66	0.0512	0.0476	0.0441	0.6698	0.6647	0.6596
97.0	3	113	0.0515	0.0490	0.0467	0.7791	0.7760	0.7730
145.4	3	159	0.0513	0.0494	0.0476	0.8297	0.8276	0.8255
193.9	3	205	0.0503	0.0488	0.0473	0.8590	0.8575	0.8559

Table 5 shows the optimal c values according to various values of offered load $\overline{g}\lambda/\mu$ and the corresponding optimized BU, where n = 16; Cp_c = 5%; μ = 0.00125; λ ranges from 0.00625 to 0.05; the arriving group size was distributed with GEOM (please refer to Table 2 for the normalized probabilities.), and π varies from 1 to 3 ($\overline{g}$ = 6.17, 5.01 and 4.85, respectively). The BU falls when c is increased to 1 more than the optimal value. Conversely, the CBP exceeds the

constraint C_{Pc} when c is 1 less than its optimal value. Hence the table presents the optimal values of c. In the OVSF multi-code assignment system, the optimal c for maximizing BU can be considered to set about c basic-rate codes in the corresponding Node-B. Restated, the Node-B should be assigned the corresponding frequency bandwidth to support the c codes.

6. CONCLUSION

This paper demonstrates the effectiveness of the batch-arrival model $M^{\phi(X)}/M/c/c$ for analyzing the OVSF multi-code assignment performance. The CBP and BU are two important performance measures in the multi-code assignment system, which respectively represent the quality of service for subscribers and the profit of operators. The simulation results agree with the predictions derived from the proposed model, indicating that the model successfully evaluates the system. Additionally, operators will be able to apply the measures obtained to the utilization maximization problem that finds the optimal number of OVSF codes in a Node-B to gain the maximum profit with a specific QoS constraint. The model should be useful for constructing WCDMA networks.

REFERENCES

3GPP (2007). Spreading and modulation (FDD) (Release 7), TR25.213, v7.4.0.

Wan, C. S., Shih, W. K., & Chang, R. C. (2003). Fast dynamic code assignment in next generation wireless access networks. *Computer Communications*, *26*, 1634-1643.

Adachi, F., Sawahashi, M., & Suda, H. (1998). Wideband CDMA for next generation mobile communications systems. *IEEE Communications Magazine*, *36*(9), 56-69.

Yen, L. H., & Tsou, M. C. (2004). An OVSF code assignment scheme utilizing multiple RAKE combiners for W-CDMA. *Computer Communications*, *27*, 1617-1623.

Chao, C. M., Tseng, Y. C., & Wang, L. C. (2005). Reducing internal and external fragmentations of OVSF codes in WCDMA systems with multiple codes. *IEEE Transactions on Wireless Communications*, *4*(4), 1516-1526.

Lee, S. J., Lee, H. W., & Sung, D. K. (1999). Capacities of single-code and multicode DS-CDMA systems accommodating multiclass services. *IEEE Transactions on Vehicular Technology*, *48*(2), 376-384.

Karakoc, M., & Kavak, A. (2007). A New Dynamic OVSF Code Allocation Method based on Adaptive Simulated Annealing Genetic Algorithm. *Proceedings of IEEE 18th International Symposium on Personal, Indoor and Mobile Radio Communications (PIMRC 2007)*, 1-5.

Cruz-Perez, F. A., Vazquez-Avila, J. L., Seguin-Jimenez, A., & Ortigoza-Guerrero, L. (2006). Call admission and code allocation strategies for WCDMA systems with multirate traffic. *IEEE Journal on Selected Areas in Communications*, *24*(1), 26-35.

Chen, M. X., & Hwang, R. H. (2006). Efficient OVSF code assignment and reassignment strategies in UMTS. *IEEE Transactions on Mobile Computing*, *5*(7), 769-783.

Jui-Chi Chen received his B. S. (1993) and M. S. (1995) in Computer Science and Information Engineering from National Chao Tung University and Ph. D. (2006) in Computer Science from National Chung Hsing University. He is currently an Assistant Professor in the Department of Computer Science and Information Engineering of Asia University, Taiwan. His research interests include wireless communications and computer networks.

Hui-Fuang Ng received his B. S. (1988) in Agricultural Machinery Engineering from National Chung Hsing University and M. S. (1993) and Ph. D. (1996) in Biosystems and Agricultural Engineering from University of Minnesota, USA. He is currently an Assistant Professor in the Department of Computer Science and Information Engineering of Asia University, Wufeng, Taiwan. His current research interests include computer vision, image processing and pattern recognition.

Hsin-Li Lin received his B. S. degree in Biology from National Taiwan University in 1971; Ph. D. degree in biomedicine from University of Texas at Houston in 1979; and M. S. degree in Computer Science from Johns Hopkins University in 1983. Since then he had spent over 20 years in several research organizations and business enterprises in United States in research and management capacities, including National Institute of Health (NIH), MITRE Corp., GTE Corp, Hughes Network Systems Corp., and Cheetah Global Communications Corp. During

this time period he had headed and successfully implemented several large international projects such as wireless fixed telephone system in Brazil, wireless mobile phone system and wireless data communications system in China, and broadband microwave transmission system in Taiwan. He joined Asia University as joint professor in Department of Computer Science and Information Engineering, Department of Biotechnology, and Department of Bioinformatics since 2005. His research interest concentrates on the innovative applications of modern information technologies on biomedical, educational, and business enterprise issues and had published many conference and journal papers on various topics.